

A Study of Manipulator with Passive Revolute Joint

Asaji SATO¹, Osamu SATO², Nobuya TAKAHASHI², and Michio KONO²

¹Dept. of Mechanical Engineering, Miyakonojo National college of Technology, Miyakonojo 885-8567, Japan.

²Dept. of Computer Science and Systems Engineering, Faculty of Engineering, University of Miyazaki, Miyazaki 889-219, Japan.

Abstract: In this paper, equations of motion of a manipulator, whose mechanism has a passive revolute joint, are derived in consideration of characteristics of driving source. Considering the final condition about displacement and velocity of the passive joint, trajectories of velocity for saving energy are calculated by iterative dynamic programming. And, the dynamic characteristics of manipulator controlled based on the trajectory for saving energy are analyzed theoretically.

Keywords: Manipulator, Trajectory, Dynamic Programming, DC Motor, Minimum Energy, Passive joint.

1 Introduction

For the purpose of enlarging the work space, it is necessary for studying the optimal control of the manipulator whose mechanism has a passive joint. In a previous report [1], a casting manipulator is introduced, and it has large work space compared with its simple mechanism. But, the consideration of energy consumption is not enough. In horizontal plane, obstacle avoidance motion planning for a three-axis planar manipulator with a passive joint is investigated [2]. But, energy consumption is not considered.

In previous report by the authors [3], trajectories for saving energy of manipulator, whose mechanism has two active joints, were easily calculated by iterative dynamic programming.

In this paper, equations of motion of a manipulator, whose mechanism has a passive revolute joint, are derived in consideration of the characteristics of DC servomotors, and a performance criterion for saving energy is defined in consideration of energy consumption of the driving source. When the manipulator is operated in a vertical plane, the system is highly non-linear due to gravity, and an analytical solution can not be found. Then, a numerical approach is necessary. Considering the final condition about displacement and velocity of the passive joint, the trajectories of velocity for energy saving are calculated by iterative dynamic programming. Initial searching region, which is parallel, is shifted to minimize the energy consumption of the motor. The dynamic characteristics of manipulator controlled based on above mentioned trajectory are analyzed theoretically and investigated experimentally.

2 Modeling of manipulator with passive joint

The dynamic equations of the manipulator with

three degrees of freedom as shown in Figure 1, which is able to move in a vertical plane, are as follows.

$$\begin{bmatrix} A_{11} & A_{12} & A_{13} \\ A_{21} & A_{22} & A_{23} \\ A_{31} & A_{32} & A_{33} \end{bmatrix} \begin{bmatrix} \ddot{\theta}_1 \\ \ddot{\theta}_2 \\ \ddot{\theta}_3 \end{bmatrix} = \begin{bmatrix} \tau_1 - \tau_2 + A_{14} \\ \tau_2 - \tau_3 + A_{24} \\ \tau_3 + A_{34} \end{bmatrix} \quad (1)$$

where

$$A_{11} = a_1 + a_4 C_2 + a_6 C_{23}, A_{12} = a_4 C_2 + a_6 C_{23}, A_{13} = a_6 C_{23},$$

$$A_{14} = a_4 (\dot{\theta}_1 + \dot{\theta}_2)^2 S_2 + a_6 (\dot{\theta}_1 + \dot{\theta}_2 + \dot{\theta}_3)^2 S_{23} - a_7 C_1,$$

$$A_{21} = a_2 + a_4 C_2 + a_5 C_3, A_{22} = a_2 + a_5 C_3, A_{23} = a_5 C_3,$$

$$A_{24} = -a_4 \dot{\theta}_1^2 S_2 + a_5 (\dot{\theta}_1 + \dot{\theta}_2 + \dot{\theta}_3)^2 S_3 - a_8 C_{12},$$

$$A_{31} = a_3 + a_5 C_3 + a_6 C_{23}, A_{32} = a_3 + a_5 C_3, A_{33} = a_3,$$

$$A_{34} = -a_5 (\dot{\theta}_1 + \dot{\theta}_2)^2 S_3 - a_6 \dot{\theta}_1^2 S_{23} - a_9 C_{123},$$

$$a_1 = I_{G1} + m_1 r_1^2 + m_2 l_1^2 + m_3 l_1^2,$$

$$a_2 = I_{G2} + m_2 r_2^2 + m_3 l_2^2, a_3 = I_{G3} + m_3 r_3^2,$$

$$a_4 = m_2 l_1 r_2 + m_3 l_1 l_2, a_5 = m_3 l_2 r_3, a_6 = m_3 l_1 r_3,$$

$$a_7 = (m_1 r_1 + m_2 l_1 + m_3 l_1) g,$$

$$a_8 = (m_2 r_2 + m_3 l_2) g, a_9 = m_3 g r_3,$$

$$C_1 = \cos \theta_1, C_2 = \cos \theta_2, C_3 = \cos \theta_3,$$

$$S_1 = \sin \theta_1, S_2 = \sin \theta_2, S_3 = \sin \theta_3,$$

$$C_{12} = \cos(\theta_1 + \theta_2), C_{23} = \cos(\theta_2 + \theta_3),$$

$$S_{12} = \sin(\theta_1 + \theta_2), S_{23} = \sin(\theta_2 + \theta_3),$$

$$C_{123} = \cos(\theta_1 + \theta_2 + \theta_3), S_{123} = \sin(\theta_1 + \theta_2 + \theta_3).$$

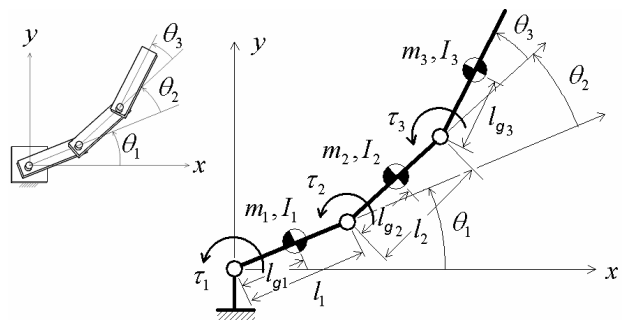


Fig.1 Mechanism of manipulator

We shall take the parameters of the system as shown in Table 1. The simulations of the system are done as follows. The angular frequency of pendulum movement are approximated as

$$\omega_2 \cong \sqrt{\frac{m_2 g l_{g2} + m_3 g l_2}{I_{G2} + m_2 l_{g2}^2 + m_3 l_2^2}} \cong 11.07 \text{ (rad/s)} \quad (2)$$

$$\omega_3 = \sqrt{\frac{m_3 g l_{g3}}{I_{G3} + m_3 l_{g3}^2}} \cong 12.8 \text{ (rad/s)} . \quad (3)$$

Then, output torques of the motor are

$$\begin{aligned} \tau_1 &= 0, \quad \tau_2 = A_2 \sin(\omega_2 t), \quad \tau_3 = A_3 \sin(\omega_3 t), \\ A_2 &= 0.006 \text{ (Nm)}, \quad A_3 = -0.003 \text{ (Nm)} . \end{aligned} \quad (4)$$

A response of the manipulator from initial position $[\theta_{1i} = (-\pi/2), \theta_{2i} = 0, \theta_{3i} = 0]$ is shown in Figure 2.

By inertia force, amplitude of pendulum movement increases as the response time increases.

3 Upward circling motion of manipulator

The applied voltage of the servomotor is

$$e_j = b_{1j} \dot{\theta}_j + b_{2j} \ddot{\theta}_j + b_{3j} \tau_j + b_{3j} \tau_{fj} \text{sign}(\dot{\theta}_j) \quad (5)$$

where

$$b_{1j} = k_{vj} + (R_{aj} / k_{ij}) D_{mj}, \quad b_{2j} = (R_{aj} / k_{ij}) I_m, \quad b_{3j} = R_{aj} / k_{ij},$$

i_{aj} : electric current of the armature ,
 R_{aj} : resistance of armature ,
 I_m : moment of inertia of armature,
 D_{mj} : coefficient of viscous damping.

Then, the electric current is

$$i_{aj} = (e_j - k_{vj} \dot{\theta}_j) / R_{aj} . \quad (6)$$

And, the consumed energy is

$$E = \sum_{j=1}^3 \int (e_j \cdot i_{aj}) dt . \quad (7)$$

Under the condition that joint 1 is passive, ($\tau_1 = 0$), the simulations of the system are down as follows.

Figure 3 shows a flow chart for iterative dynamic programming method. In frame (A), the trajectory for saving energy is searched by dynamic programming [3]. In frame (B), the searching region is shifted to minimize the consumed energy, and width of the region is changed smaller. Figure 5 shows the trajectory for searching, and the initial trajectory for searching is expressed as

$$\begin{aligned} (0 \leq t \leq t_R) \quad & \theta_j = A_j t^2 \sin(\omega_j \cdot t), \\ (t_R \leq t) \quad & \theta_j = \theta_{jR} . \end{aligned} \quad (8)$$

Considering the pendulum movement in Fig.2, the reference time t_R is selected as 0.74 (s). The boundary conditions are $\theta_j(t_R) = \theta_{jR}$, $\dot{\theta}_j(t_R) = 0$. And then,

$$2A_j t_R \sin(\omega_j t_R) + \omega_j A_j t_R^2 \cos(\omega_j t_R) = 0 , \quad (9)$$

$$A_j = \left[\theta_{jR} / \left\{ t_R^2 \cdot \sin(\omega_j t_R) \right\} \right] . \quad (10)$$

Under the condition that $\theta_{2R} = 3.0, \theta_{3R} = 1.1$ (rad), the angular velocity and the amplitude are calculated as $\omega_2 = 10.9, \omega_3 = 15.2$ (rad/s), $A_2 \cong 5.64, A_3 \cong -2.06$.

This proposed trajectory is used as a center line of initial searching region of the iterative dynamic programming.

Table 1 Parameters of the manipulator

Parameter	Value	Parameter	Value
l_1 (m)	0.08	l_{g1} (m)	0.04
l_2, l_3 (m)	0.09	l_{g2}, l_{g3} (m)	0.045
I_{G1} (kg·m ²)	1.07×10^{-5}	m_1, m_2, m_3 (kg)	0.02
I_{G2}, I_{G3} (kg·m ²)	1.35×10^{-5}	k_{t2}, k_{t3} (Nm/A)	0.046
D_{m2}, D_{m3} (Nms/rad)	7.9×10^{-5}	k_{v2}, k_{v3} (Vs/rad)	0.046
τ_{f2}, τ_{f3} (Nm)	0.0013	R_{a2}, R_{a3} (Ω)	3.5

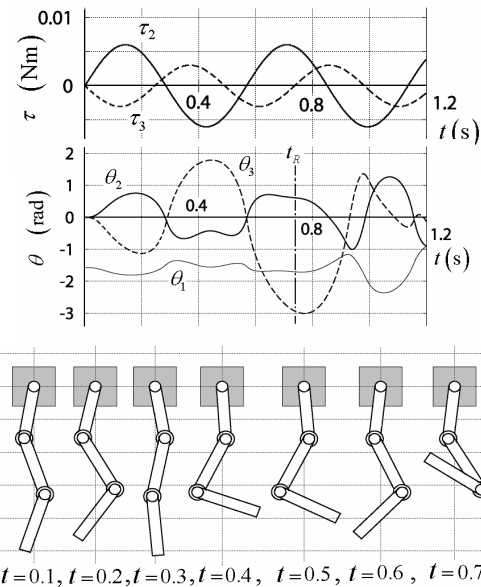


Fig.2 Response of manipulator with a passive joint

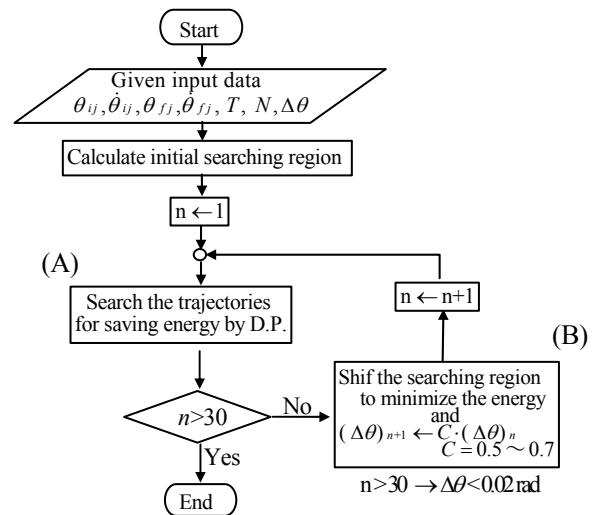


Fig.3 Flow chart for simulation

Figure 4 shows the solutions of Eq.9, and Figure 5 shows the trajectory for searching. We shall take the parameters of the system as shown in Table 1.

A response of the manipulator from the initial position $(\theta_{1i} = -\pi/2, \theta_{2i} = 0, \theta_{3i} = 0)$ to the final position $[\theta_1(t_f) = 1.3, \theta_2(t_f) = 3.0, \theta_3(t_f) = 1.1 \text{ rad}]$ is shown in Fig.6, under the condition that working time $t_f = 1.2 \text{ (s)}$. In this case, joint 1 is passive, and joint 2, 3 are actuated. In Figure 6, it is shown that link 1 arrived at desired position $\theta_1(t_f)$. And the motion is caused by inertia force of pendulum movement of link 2 and 3.

Figure 7 shows a locus of the center of gravity about the motion of Fig.6.

The dynamic equation of the manipulator is rearranged for $\tau_1 = 0$, and

$$\begin{bmatrix} A_{11} & 1.0 & 0 \\ A_{21} & -1.0 & 1.0 \\ A_{31} & 0 & -1.0 \end{bmatrix} \begin{bmatrix} \ddot{\theta}_1 \\ \tau_2 \\ \tau_3 \end{bmatrix} = \begin{bmatrix} A_{14} - A_{12}\ddot{\theta}_2 - A_{13}\ddot{\theta}_3 \\ A_{24} - A_{22}\ddot{\theta}_2 - A_{23}\ddot{\theta}_3 \\ A_{34} - A_{32}\ddot{\theta}_2 - A_{33}\ddot{\theta}_3 \end{bmatrix} \quad (1')$$

The angular acceleration of joint 2, 3 are given in iterative dynamic programming method, and the angular acceleration of joint 1 and torques of joint 2, 3 are calculated simultaneously.

Figure 8 shows the torques of joint 2, 3 which are necessary for actuating the link 2 and 3. In Figure 8 and 9, it is shown that torques increase at 0.6~0.7 (s), and the consumed energy of the motors increase too.

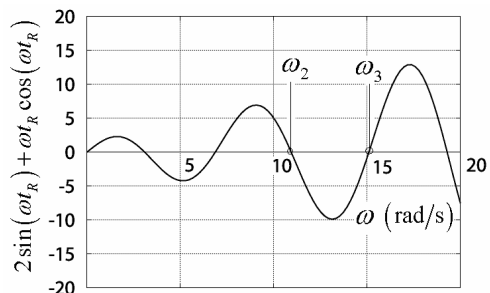


Fig.4 Angular velocity (calculated by Eq.9.)

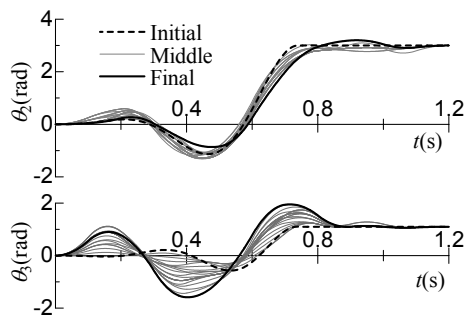


Fig.5 Trajectory for searching

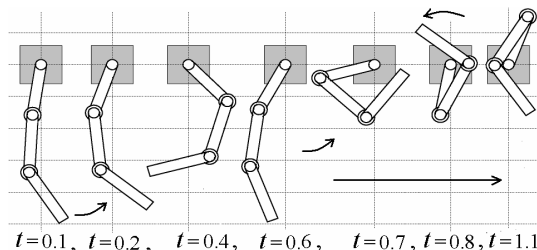
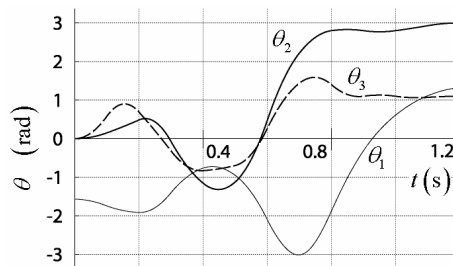


Fig.6 Upward circling motion of manipulator

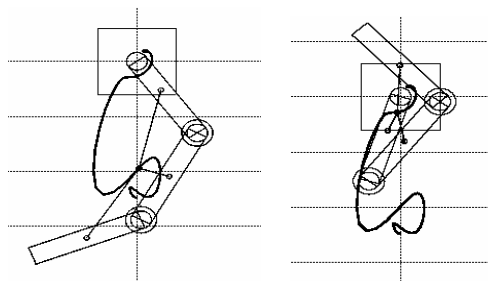


Fig.7 Locus of the center of gravity

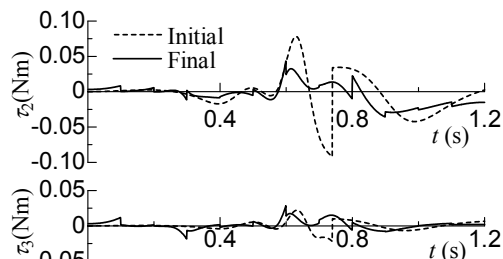


Fig.8 Torque of the motor

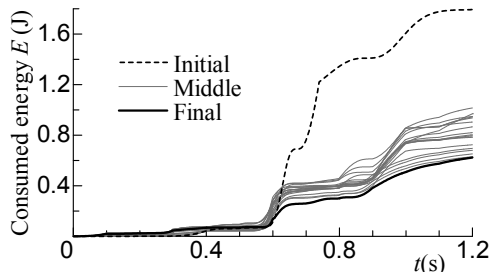


Fig.9 Consumed energy of the motors

4 Experimental results

In this section, the results of fundamental experiment are shown to examine the effectiveness of modeling for the simulations.

Figure 10 shows an experimental apparatus, which is used in previous report by the authors [3]. A tray (link 3) is connected to link 2 by a passive revolute joint.

Under the condition that the torque of joint 3 is zero, the angular acceleration of joint 1 and 2 are given in iterative dynamic programming method, and the acceleration of link 3 and torques of joint 1, 2 are calculated simultaneously. Figure 11 shows a mechanism of manipulator whose mechanism is a closed type.

The parameters of the system are shown in Table 2. The motors 1 and 2 (rated 24 V, 60W) are on the frame, and sampling time of the control is 0.002 [s]. The feedback gain for angular displacement is 50[V/rad], the feedback gain for angular velocity is 0.5[V/s/rad].

Figure 12 shows the experimental response, under the condition that initial position is $(\theta_{1i} = \theta_{2i} = -\pi/4, \theta_{3i} = 0)$, the final position is $(\theta_{1f} = \pi/2, \theta_{2f} = -\pi/4, \theta_{3f} = \pi/4)$, and the working time is 0.8 [s]. Figure 12(a), (b) show the experimental response of angular velocity of motor which are calculated by angular displacement measured by rotary encoder. Broken line is theoretical result, and solid line is experimental result. In Figure 12(c), it is shown that link 3 is arrived at desired position. And the motion is caused by inertia force of link 1 and 2. And, Fig.12 (d), (e) are applied voltage and electric current of motor 1. The theoretical result is similar to the experimental one.

5 Conclusions

The results obtained in this paper are summarized as follows.

- (1) It is considered that the trajectory for saving energy of manipulator with passive revolute joint is available for the work in vertical plane.
- (2) From experimental results, it is considered that modeling for simulation is effective.

References

[1] H.Arisumi, K.Yokoi, T.Kotoku et al (2002), Casting Manipulation (Experiments of Swing and Gripper Throwing Control), International Journal of JSME, Vol.45, No.1 C, pp.267-274.
 [2] N. Shiroma, K.M.Lynch, H.Arai and K.Tanie (2000), Motion Planning for a Three-Axis Planar Manipulator with a Passive Revolute Joint, Journal of JSME (in Japanese), Vol.66, No.642, pp.545-552.
 [3] A.Sato, O.Sato, N.Takahashi and M.Kono (2006), Trajectory for Saving Energy of Direct-Drive Manipulator in Throwing Motion, Proc. of AROB 11th, pp.783-786.

Table 2 Parameters of experimental apparatus

Parameter	Value	Parameter	Value
I_{G1}, I_{G4} (kg·m ²)	1.73×10^{-5}	m_1, m_4 (kg)	0.0202
I_{G2} (kg·m ²)	8.42×10^{-5}	m_2 (kg)	0.078
I_{G3} (kg·m ²)	9.43×10^{-6}	m_3 (kg)	0.0182
I_{G5} (kg·m ²)	2.04×10^{-5}	m_5 (kg)	0.0218
l_{g1}, l_{g4}, l_{g5} (m)	0.04	l_1, l_4, l_5 (m)	0.08
l_{g2} (m)	0.0468	l_2 (m)	0.115
l_{g3} (m)	0.03	l_3 (m)	0.05

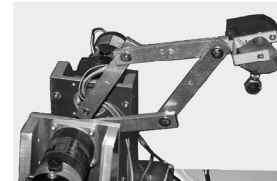


Fig.10 Experimental apparatus

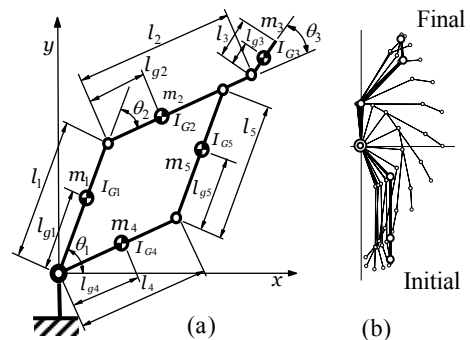


Fig.11 Mechanism of manipulator

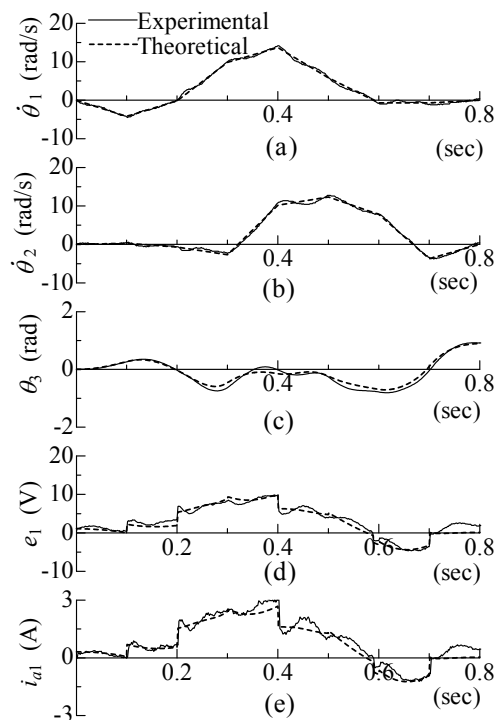


Fig.12 Experimental results